Chalcopyrite Dissolution: Challenges

Denise Bevilaqua, Ailton Guilherme Rissoni Toledo, Laíze Guimarães Crocco, Riberto Nunes Peres, Rachel Biancalana da Costa, Assis Vicente Benedetti and Olli H. Tuovinen

Abstract

Chalcopyrite is the main source of copper in the world, amounting to nearly 70% of the copper reserves. Nonetheless, chalcopyrite is highly recalcitrant to chemical and biological processing for copper extraction. Concentration by flotation and Cu recovery by pyrometallurgical techniques are still the main route for processing chalcopyrite concentrates, although they are unfeasible for copper extraction from low-grade ores that make up the most copper reserves. Acid bioleaching is a promising technique for extracting copper from low-grade copper ores, and the technology has been studied for decades, but there is still no commercial-scale bioleaching application for copper recovery from chalcopyrite concentrates. Bioleaching is practiced with low-grade chalcopyrite ores in heap leaching processes with ores of multiple sulfide minerals. Research in this area has probed electrochemical reactions, biological activities, and interactions with microbes and mineral surfaces to integrate operational models for chalcopyrite bioleaching. The purpose of this chapter is to review the evolution in the understanding of the chemical leaching and bioleaching of chalcopyrite in the last 20 years, and the progress achieved so far.

Keywords

Chalcopyrite bioleaching · Electrochemical techniques · Galvanic interactions · Redox potential control · Polarization

1 Introduction

Copper ranks as the third most consumed metal in the world, and its consumption has been increasing consistently with the industry and technology. Copper has a wide range of industrial and consumer applications due to its high thermal and electrical conductivity and the propensity to form metallic alloys with many other metals. Global demand for copper continues to increase because it plays an indispensable role in modern technologies including applications in renewable energy areas. About 70% of the global copper reserves are chalcopyrite ($CuFeS_2$) ores, and 70–80% of copper production comes from this mineral (Nyembwe et al., 2018).

Chalcopyrite is a recalcitrant mineral in hydrometallurgy, characterized by slow dissolution kinetics. Flotation and pyrometallurgical techniques are still the main route for processing chalcopyrite, although they are economically unfeasible for copper extraction from low-grade ores, which constitute the most copper reserves. Several chemical and biological strategies have been proposed to improve copper solubilization from chalcopyrite. Chemical alternatives in hydrometallurgy include for example process adjustments with catalytic ions, controlled redox potential, and use of ferrous and ferric iron and chloride to modify the leach solution. Hydrogen peroxide, Na-nitrate, Cr^{6+}, and Cu^{2+} have also been tested as chemical oxidants (Li et al., 2013), but their best use may be in the elucidation of the mechanisms and steps on chalcopyrite oxidation. As predicted from the Van't Hoff equation, temperature in the range of ambient to 120 °C in autoclaves is efficient in enhancing

D. Bevilaqua (✉) · A. G. R. Toledo · L. G. Crocco · R. B. da Costa
Department of Biochemistry and Organic Chemistry, Institute of Chemistry, São Paulo State University (UNESP), Araraquara, SP 14800-060, Brazil
e-mail: denise.bevilaqua@unesp.br

R. N. Peres · A. V. Benedetti
Department of Analytical, Physical-Chemical and Inorganic Chemistry, Institute of Chemistry, São Paulo State University (UNESP), Araraquara, SP 14800-060, Brazil

O. H. Tuovinen
Department of Microbiology, Ohio State University, 484 West 12th Avenue, Columbus, OH 43210, USA

S. Panda et al. (eds.), *Biotechnological Innovations in the Mineral-Metal Industry*, Advances in Science, Technology & Innovation, https://doi.org/10.1007/978-3-031-43625-3_2

the kinetics of chemical leaching of chalcopyrite. Many advances in biological strategies were achieved in the late twentieth century, leading to greatly increased knowledge of physiological capabilities of acidophilic microorganisms for chalcopyrite solubilization. Some processes with chalcopyrite concentrates were advanced to pilot scale and also demonstrated at a large scale (Watling, 2013), but commercialization has not materialized. Thus, bioleaching processes are yet to develop to economically competitive technology for copper extraction from chalcopyrite concentrates. Heap leaching applications of low-grade ores that contain chalcopyrite typically also contain secondary copper and other metal sulfides, which are more readily subjected to dissolution. An example of polymetal sulfide ore extraction is the Terrafame heap leaching operation (www.terrafame.com) in NE Finland. The operation recovers Zn, Ni, Co, Cu, and U in the acid leach cycle, and a second leach cycle with extended residence time is practiced accommodating the slow dissolution of Cu from chalcopyrite and U from thucholite in secondary bioleaching heaps.

This chapter addresses the refractoriness of chalcopyrite dissolution and the role of microorganisms in chalcopyrite bioleaching. The chapter emphasizes electrochemical techniques inasmuch as they help to elucidate the mechanisms of chalcopyrite dissolution. The redox potential as a strategy to promote chalcopyrite dissolution is also appraised in this chapter.

2 Chalcopyrite Properties and Models to Explain the Refractoriness

The lattice energy of chalcopyrite is close to 17,000 kJ mol^{-1}, and the standard enthalpy of formation ΔH_f and the standard Gibbs free energy of formation ΔG_f° values are −193.6 and −190.6 kJ mol^{-1}, respectively. These ΔH_f and ΔG_f° values are in the common range for sulfide minerals and do not explain the recalcitrance and unfavorable kinetics of chalcopyrite dissolution (Li et al., 2013).

Slow dissolution of chalcopyrite has been recognized through the years (e.g., Dutrizac, 1978, 1991; Nicol et al., 2017; Nicol, 2017a, 2017b; Viramontes-Gamboa et al., 2006, 2007, 2010). The slow dissolution has been mainly attributed to the formation of passive, metal-depleted layers on chalcopyrite surface and to chalcopyrite properties as semiconductor material (Crundwell, 1988; Liu & Li, 2011; Weisener et al., 2003; Yu et al., 1973).

Potential measurements have been used to analyze chalcopyrite passivation. The increase in the current with positive potentials is considered to signal a transpassive phenomenon. Transpassivation is a phenomenon, in which a passivated surface (metal, metal alloys, or mineral) begins to dissolve fast when the electrode potential becomes too positive and surpasses the breakdown potential of the passive film. According to Nicol (2017b), the formation of a transpassive region and the oxidation of chalcopyrite in sulfate solutions occur at lower potentials than in chloride solutions. Nicol (2017a) reported that the capacitance values vary with the applied potential, decreasing between 0.40 and 0.95 V_{SHE} in 0.3 mol L^{-1} sulfuric acid and sharply increasing with potentials > 1 V_{SHE}, thus manifesting a trend similar to the measured current. These results support the findings that intermediate solid-phase products are formed on chalcopyrite between 0.4 and 0.95 V_{SHE}, causing the formation of a passivation layer, which hinders further dissolution.

Both Fe^{3+} and Cu^{2+} act as oxidants in the leaching of chalcopyrite in chloride-containing solutions (Nicol & Zhang, 2017). Potentiostatic measurements (current vs. time) showed that the potential region between 0.65 and 0.80 $V_{Ag|AgCl|KCl(3\ mol\ L^{-1})}$ is important in the electrochemical leaching process. The authors also reported slow dissolution of chalcopyrite even after 24 h. Different concentrations of chloride did not influence chalcopyrite leaching, whereas the pH and specific potentials (0.65–0.80 V) in chloride-containing solutions had major effects (Nicol & Zhang, 2017). In contrast, Bevilaqua et al. (2013) demonstrated that the addition of 0.10–0.20 mol L^{-1} NaCl enhanced both the chemical leaching and bacterial leaching of chalcopyrite in shake flasks and stirred tank bioreactor conditions at mesophilic temperatures. The highest rate chalcopyrite leaching occurred at < 0.45 $V_{Ag|AgCl|KClsat}$ redox potential (Bevilaqua et al., 2013). Chloride ions inhibit the formation of secondary solid phases from chalcopyrite, decreasing the precipitation of ferric iron as jarosite-type secondary phases (Vakylabad et al., 2022). Secondary Cu-sulfides and S^0 are also decreased, sometimes below the detection by X-ray diffraction analysis of solid residues (Bevilaqua et al., 2013). Thus, chloride ions decrease the passivation of chalcopyrite (Martins et al., 2019, Martin & Leão, 2023). Chloride toxicity at the > 0.2–0.3 mol L^{-1} range may, however, impede the bioleaching action depending on the microbial culture (Akcil et al., 2013; Dopson et al., 2017; Huynh et al., 2019). Several halotolerant iron- and sulfur-oxidizers have been described, some tolerating chloride concentrations above the ~ 0.5 mol L^{-1} in seawater (Zammit et al., 2012; Khaleque et al., 2018; Martins et al., 2019, Martin & Leão, 2023). Wang et al. (2022) reviewed prospects of using seawater-based lixiviants in heap leaching systems. The toxicity of seawater, ~ 0.5 mol L^{-1} Cl^- with ~ 35‰ salinity, in heap bioleaching systems necessitates testing, selection, and acclimatization for salt-tolerant microbial communities.

Chalcopyrite oxidation in alkaline solutions involves mineral activation at low potentials, followed by passivation and transpassivation at high potentials and decreasing oxidation at > 18 h of contact (Nicol, 2019). In mixed chloride

and sulfate solutions containing Fe^{3+} and Cu^{2+}, the solution potential of 0.2 $V_{Ag|AgCl|KCl(3\ mol\ L^{-1})}$ varied, and potentiostatic measurements confirmed that a specific mixed potential region supports oxidative dissolution of copper and iron from chalcopyrite (Nicol, 2021).

Zhao et al. (2019) reviewed the dissolution and passivation mechanism of chalcopyrite in the bioleaching process, pointing out that several secondary products are formed that can cause chalcopyrite passivation during the leaching process. The three main passivating products formed during contact of chalcopyrite in leach solution are S_n^{2-} (polysulfides), S^0 (elemental sulfur), and $XFe(SO_4)(OH)_6$ (jarosite-type precipitates), where X is usually mixtures of K^+, NH_4^+, H_3O^+, and Na^+. The polysulfide film formed on chalcopyrite can have a thickness of up to 1 μm and its formation is due to the dissolution of Fe^{2+}, thus leading to Fe-deficient copper polysulfides (CuS_n), which are unstable and readily converted to other Cu-sulfides (Zhao et al., 2019). Some studies suggest that polysulfides are not the main passivating agents of chalcopyrite because they are oxidized increasingly to form elemental sulfur at redox potentials of > 0.9 V_{SHE} (Klauber, 2008; Parker et al., 2003; Zhao et al., 2019). The formation of S^0 is considered as the main passivating agent in sulfate-rich and bioleaching solutions and is further oxidized to sulfate over time (Dutrizac, 1989; Khoshkhoo et al., 2014; Nava et al., 2008). Other studies indicate that the S^0-layer on chalcopyrite is porous and does not hinder the dissolution of chalcopyrite (Klauber, 2008; Klauber et al., 2001; Sasaki et al., 2012). Thus, the formation of a S^0-layer and its passivating effect on the acid leaching of chalcopyrite is a controversial subject because opposite effects have been reported. Some of the different interpretations emanate from the initial phase of chalcopyrite oxidation, which forms a layer on mineral surface of oxidic Fe(III) and metastable sulfide phases of unoxidized S and Cu, leading to passivation. As the leaching reactions continue, more Fe is extracted from chalcopyrite surface layers, and solid-state diffusion becomes increasingly rate controlling. Intermediate Cu-sulfide phases of the stoichiometry of chalcocite (CuS_2) and idaite (Cu_5FeS_6) have been detected on passivated chalcopyrite surfaces (Varotsis et al., 2022). Several studies suggest that jarosite-type precipitates are the main secondary phase that passivates chalcopyrite leaching: i.e., precipitation of poorly soluble Fe(III)-sulfates together with enrichment of phases with Cu–S bonds (Sandström et al., 2005; Zhao et al., 2019).

The importance of the secondary phases hindering chalcopyrite dissolution is on debate. The slow dissolution of chalcopyrite may be linked to other factors such as the structure of chalcopyrite and its semiconductor behavior. O'Connor and Eksteen (2020) have expressed strong criticism about the use of the "passivation" term. "Passivation" is not universally accepted, most likely due to its superficial resemblance, if any, to the well-known passivation behavior of metals and metal alloys, and the lack of a clearly identifiable surface layer. Several reports use the term to explain the slow chalcopyrite dissolution without the necessary scientific and analytical basis. The products formed on the mineral surface are variations of metal-deficient phases such as Fe-deficient polysulfides or sulfides, but all with the same structure and behavior (O'Connor & Eksteen, 2020).

Passivation is normally defined for metals and alloys, as discussed and explained in the literature (Fontana, 1987; Sedriks, 1996; Uhlig, 1978). The term and its derivatives in mineral studies were adopted from corrosion research and were not originally defined for minerals. A passive surface presents an appreciable and nobler potential than a non-passive surface and has a low current density due to the proximity of anodic and cathodic potentials for heterogeneous materials as well as a significant potential region with very small current up to the passive film breakdown, typically as shown in Fig. 1a. Figure 1a is different from the polarization curves observed for minerals as shown in Fig. 1b. As mentioned by O'Connor and Eksteen (2020), there are differences

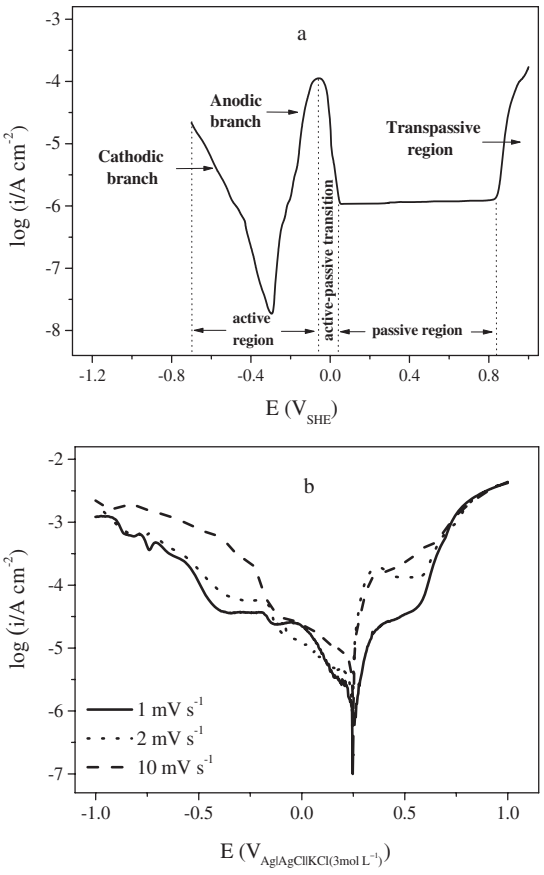

Fig. 1 Schematic representation of polarization curves: (**a**) a generic curve with characteristic parameters and specific regions; (**b**) chalcopyrite in salt leach solution (ionic strength = 0.08 mol L^{-1}) scanned at different scan rates

in passivation characteristics between metals/alloys and chalcopyrite. The mineral behavior is different from the passivation of metals, and the active–passive–transpassive regions are generally not obvious (O'Connor & Eksteen, 2020). This can be seen at different scan rates as shown in Fig. 1b. The tests performed at low scan rate (0.1 up to 10 mV s^{-1}) do not show a passivation region with low dissolution current. Sulfur species on polarized, metal-deficient chalcopyrite surface assent with interfacial mineral-leach solution species (Ram et al., 2020). Passivation and critical current density for metals tend to decrease at low pH values, but this is not observed for chalcopyrite, because its passivation can also be related to its electrochemical properties.

Mikhlin et al. (2017) analyzed the near-surface region of an oxidized chalcopyrite sample that was conditioned in acid ferric sulfate solution for 30 min at 50 °C. The group used X-ray photoelectron spectroscopy (XPS), X-ray absorption near-edge spectroscopy (XANES), and density functional theory (DFT) calculations to describe the oxidized, metal-depleted regions in the layer. Mikhlin et al. (2004, 2017) analyzed three metal-depleted layers: (i) a thin (1–4 nm) outmost layer containing polysulfide species, (ii) a ~ 20 nm thick, highly metal-deficient layer rich in disulfides but negligible in polysulfides, and (iii) a defective and near-stoichiometric underlayer of about 100 nm thickness. The slow chalcopyrite dissolution was attributed to metal depletion on chalcopyrite surface and slow diffusion of copper and iron species from the bulk solid to the mineral surface (Mikhlin et al., 2004, 2017).

Mikhlin et al. (2004) determined the capacity of non-stoichiometric sulfides and intermediates from chalcopyrite, bornite (Cu_5FeS_4), and chalcocite (Cu_2S) to passivate their surfaces. Covellite (CuS) was not formed on the oxidation of chalcopyrite, whereas the formation of non-stoichiometric sulfides ($Cu_{1-x}Fe_{1-y}S_{2-z}$, Cu_xS) was confirmed (Mikhlin et al., 2004). Chalcopyrite oxidation yielded copper and iron in the solution phase and the formation of S–S bonds on the mineral surface. The sulfur/metal and copper/iron ratios in the aqueous phase were dependent of the potential that was applied. The non-stoichiometric layers on chalcopyrite surface were not the cause of passivation. Mikhlin et al. (2004) concluded that the low chalcopyrite dissolution was due to the extremely slow diffusion of copper and iron from the bulk solid to the chalcopyrite surface (i.e., metal depletion). Thus, the slow chalcopyrite dissolution was associated with the semiconductor behavior or the formation of passive layer on chalcopyrite surface.

Nasluzov et al. (2019) demonstrated in DFT + U (U = Hubbard-type correction parameter) simulation and chalcopyrite XPS studies that the crystal structure comprises centers with tri- or pentasulfide or tri- and disulfide complex anions, with a negative energy formation of 1.2–1.5 eV for each Fe atom extracted from the structure. The XPS data suggested initial depletion of iron, but not copper, on chalcopyrite surface and the presence of sulfides and polysulfide anions (S_n^{2-} with $n > 5$). During chalcopyrite oxidation, Cu was depleted as S–S chains were formed. The stability of the polysulfide centers was considered responsible for the delayed oxidation and leaching of chalcopyrite (Nasluzov et al., 2019).

Contrary to the conclusions suggested by Mikhlin et al. (2004), Zhao et al. (2015a, 2019) reported bornite and covellite as the main intermediates associated with chalcopyrite dissolution. Bornite formation represented a reductive step, which was believed to be a rate-limiting reaction in the overall chalcopyrite dissolution. Covellite formation from bornite was an oxidation step and not a cause of the rate limitation (Zhao et al., 2019).

The contrasting interpretations may be attributed to the differences in chalcopyrite surface characterization, although the surfaces were characterized in cyclic voltammetry experiments in both studies. It is possible that due to experimental differences, atypical secondary solid phases with variable stability were formed in the two studies. This controversy shows, however, that multiple experimental and analytical approaches should be used to interpret the formation of intermediate solid phases during the time course of chalcopyrite dissolution.

In the semiconductor model of chalcopyrite and leaching, the path of electron transfer between chalcopyrite and a redox pair in the solution depends on their respective energy levels (Memming, 2015). It is necessary that the energy level of the redox pairs in the electrolyte (E_{redox}) approaches the energy of the edge of the conduction band (E_C) or the valence band (E_V) of the semiconductor chalcopyrite (Crundwell, 1988; Osseo-Asare, 1992). If this condition is established, but the E_{redox} and the semiconductor Fermi level (E_F) are not at the same energy level, a charge transfer arises between the semiconductor and the redox pairs in solution in order to establish the equilibrium (Bott, 1998).

Electron transfer makes the phases negatively or positively charged. This affects the density of the states of the redox pairs, and in the case of the semiconductor, the excess or lack of charge is distributed within the solid up to a distance of about 10–1000 nm (Bott, 1998; Crundwell, 2015); this zone is called the space charge region. The space charge regions with a lack or excess of major charge carriers (electrons for n-type semiconductors and holes for p-type) are also called the depletion and accumulation regions, respectively (Bott, 1998).

The charge transfer of a semiconductor is a function of the concentration of major charge carriers. The semiconductor behaves like a metal in an accumulation condition, as there are excess charge carriers available for charge transfer. Slow reactions are expected in a depletion layer situation (Bott, 1998; Crundwell, 2015). Therefore,

according to the chalcopyrite semiconductor model, efficient leaching under accumulation conditions is expected.

O'Connor and Eksteen (2020) argued that many studies claim that chalcopyrite leaching in acidic solutions leads to passivation. However, other studies have shown no passivating effect in alkaline solutions with a complexing agent, although purportedly the same passivating species are formed on the mineral surface (O'Connor & Eksteen, 2020). If copper- or iron-oxides are naturally formed on the chalcopyrite surface, they are dissolved when immersed into acid solution, and eventually, the protection of the surface is destroyed. It is accepted that the Fe-S bond is broken more readily than the Cu–S bond and the direct decomposition of sulfide surface has a very slow rate. Surface analyses indicate that polysulfide chains of different sizes, elemental sulfur, and intermediate Cu-sulfides are formed. The *n*-type semiconductor character of chalcopyrite as determining its slow dissolution was also criticized by Nicol (2017a), attributing the observed effects to improper operation of laboratory equipment or experimental artifacts. Mikhlin et al. (2017) and Nasluzov et al. (2019) argued that the semiconductor character disappears after the modification of the first layers of the mineral surface. Ozone treatment after the bioleaching step was shown to oxidize reduced-S-containing complexes on chalcopyrite surface (Lv et al., 2021). Measurements of corrosion current densities (Tafel curves) and open-circuit potentials indicated increased reactivity of chalcopyrite after ozone treatment.

An alternative to the different approaches on chalcopyrite surface oxidation/dissolution is the reductive/dissolution route (Biegler & Horne, 1985; Hiroyoshi et al., 1997, 2000, 2001, 2004, 2008; Sandström et al., 2005; Gu et al., 2013; Zhao et al., 2015c), which is based on simultaneous electrochemical reactions occurring spontaneously under moderate acid leaching conditions. Based on this approach, Toledo et al. (2022) explained the high yield of copper recovery from a chalcopyrite concentrate sample under abiotic conditions at 1 atm and at 65 °C. The experimental variables were the initial concentration of Fe^{2+} ions and pulp density (ρ_{pulp}). Relatively high copper extractions were obtained at the initial $[Fe^{2+}]/\rho_{pulp}$ ratio of about 80, with an optimal range of solution potential maintained during almost all the time courses of 28 days. A response surface with statistical confidence of 0.997 was obtained using a central composite factorial design, allowing to reach the optimal condition with > 90% of chalcopyrite dissolution.

3 Galvanic Interaction

When dissimilar metals are immersed in a corrosive or conductive solution, there is a potential difference between the metals. If these metals are brought into contact or electrically connected, this potential difference produces a flow of charges. The corrosion of the less resistant metal increases and that of the more resistant metal decreases, compared to their behavior when they are electrically separated. Thus, the metal more resistant to corrosion acts as a cathode and the less resistant as an anode generating a galvanic cell. This behavior can be extended to other materials, for example, to ores with multiple sulfide minerals.

The electrochemical action produced by different metal reactions through a path leading to electrons and electrolytes generates a difference in potentials between the involved phases. The galvanic interaction that occurs between two minerals is caused by the different rest potentials, which lead to different electrochemical reactivities (Peters, 1977). In the case of sulfide minerals, when they come into contact with each other, they can form a galvanic cell, and thus, oxidation–reduction reactions occur, caused by the difference in the resting potentials of the mineral phases (Peters, 1977). The rest potential difference distinguishes between cathodically protected and anodically sacrificed minerals.

The rest potential indicates the electrochemical reactivity. Therefore, in the galvanic cell, the mineral with the higher resting potential is considered the nobler mineral, and the mineral with the lower resting potential is actively dissolved. Classification of common sulfide minerals in terms of their rest potentials and their mineral reactivity has been presented in the literature (Peters, 1977; Tanne & Shippers, 2021). According to Zhao et al. (2015a), the pyrite addition for chalcopyrite dissolution generates a catalytic effect that is mainly attributed to the increase in galvanic current. In this galvanic cell, pyrite is the cathodic phase, while chalcopyrite acts as the anodic phase leading to preferential dissolution (Zhao et al., 2015a). The galvanic effect of pyrite has been reported in many studies of chemical leaching and bioleaching of chalcopyrite (Li et al., 2017; Natarajan & Kumari, 2014; Olvera et al., 2014; Zheng et al., 2021).

In leaching tests with chalcopyrite and bornite in different ratios, the copper extraction was greater than 90% after 30 days in all tests containing the two minerals in a mixture (Zhao et al., 2015a). Copper dissolution was 48% at the most when the two Cu-sulfide minerals were tested separately. In the presence of *Leptospirillum ferriphilum*, the leaching of copper greatly increased when the redox potential exceeded 380 $mV_{Ag|AgCl|KClsat}$, and the dissolution almost ceased when the redox potential exceeded 480 $mV_{Ag|AgCl|KClsat}$. If the redox potential was maintained in the range (380–480 $mV_{Ag|AgCl|KClsat}$) during the time course, the bioleaching of chalcopyrite and bornite admixtures yielded high copper extraction. Similar results were obtained with chalcopyrite and pyrite mixtures, with the best results with 4:1 pyrite:chalcopyrite by weight ratios. Zhao et al. (2015a) attributed these results to the optimal

redox potential range for chalcopyrite dissolution (380–480 $mV_{Ag|AgCl|KClsat.}$), while the galvanic effect by pyrite was not considered important in this case. Chalcopyrite dissolution and pyrite activation effect were dependent on the mixing ratio.

Tanne and Shippers (2021) monitored the evolution of electric current in galvanic cells with chalcopyrite–chalcopyrite, pyrite–pyrite, and chalcopyrite–pyrite mixtures in different proportions without current disturbance (ZRA—Zero Resistance Ammeter mode). The results showed that the galvanic effect on the coupling between chalcopyrite and pyrite was relatively small. The authors speculated that chalcopyrite was too recalcitrant to dissolve during the experiment because the difference in the resting potentials between the two minerals was too small. Bioleaching results confirmed that the concentrate was leached much faster and to a greater extent when assisted galvanic bioleaching was applied. In the bioleaching assays, acidophilic microorganisms played a key role in keeping the redox potential of the solution high and may have partially oxidized electrically insulating sulfur layers. The increase in pyrite content in the mixed mineral system resulted in higher Cu recovery (Tanne & Shippers, 2021).

Hiroyoshi et al. (2000) reported that the dissolution of chalcopyrite was accelerated when the redox potential was controlled at a relatively low value. Under these conditions, chalcopyrite was reduced to Cu_2S, and its subsequent rapid dissolution yielded a high copper extraction. Thus, there are also major conflicts over topics concerning the effects of bornite or pyrite on the bioleaching of chalcopyrite. The enhancement of chalcopyrite leaching is related to these interactions between the different minerals, and the optimal region of the redox potential in mixtures of chalcopyrite and other sulfide minerals also improves the leaching.

Pathak et al. (2017) reviewed several catalysts that have been shown to enhance the bioleaching of chalcopyrite. These catalysts include metals, most notably silver (e.g., as $AgNO_3$), which precipitates as Ag_2S and Ag^0 on chalcopyrite surface, enhancing the semiconductor properties of the mineral and reducing the formation of the passivating S^0 layer on the mineral surface. Silver catalyst in the bioleaching is in flux between the solution and solid phases because Ag_2S is readily oxidized by Fe^{3+} to Ag^+ and S^0. Ag_2S also acts cathodically in contact with chalcopyrite, thus assisting the galvanic coupling effect (Yang et al., 2019; Zhao et al., 2022).

Activated carbon has also been shown to enhance the bioleaching of chalcopyrite (Ahmadi et al., 2013; Méndez et al., 2022). This effect is attributed to the activated carbon sorption of sulfur intermediates, thereby partially alleviating passivation effect caused by S^0 formation. Activated carbon is cathodic with respect to chalcopyrite, and this galvanic interaction has a positive effect in the bioleaching. It is conceivable that, as shown with biochar treatment, excessive activated carbon results in the formation of a passivating surface layer with sulfur-laden carbon intermixed with jarosite-type precipitates. Yang et al. (2017) demonstrated that visible light and 0.1% graphene accelerated Fe^{2+} oxidation during chalcopyrite bioleaching. The effect also involved jarosite precipitation on graphene particle surfaces, thus reducing its formation on chalcopyrite surface. Cyclic voltammetry results were consistent with these effects.

4 Bioleaching Microorganisms

Several bacteria and archaea capable of oxidizing Fe- and S-compounds produce acid leaching conditions for the dissolution of chalcopyrite (Latorre et al., 2016; Sadeghieh et al., 2020). They produce protons from sulfur oxidation (Eq. 1) under acidic conditions and regenerate Fe^{3+} as the chemical oxidant (Eq. 2) in the bioleaching process.

$$2S^0 + 3O_2 + 2H_2O \rightarrow 2SO_4^{2-} + 4H^+, \quad (1)$$

$$4Fe^{2+} + O_2 + 4H^+ \rightarrow 4Fe^{3+} + 2H_2O. \quad (2)$$

Rather than pure cultures, mixed cultures containing S- and Fe-oxidizers are recognized to be more efficient in the bioleaching. Many of these microorganisms are commonly found in acid mine drainage and sediments. They vary in their temperature requirements, responses to pH, and tolerance to high concentrations of metals. Several reviews have been published in the last decade on the diversity of these bacteria and archaea (e.g., Johnson & Quatrini, 2020; Mahmoud et al., 2017; Moya-Beltrán et al., 2021; Nuñez et al., 2017; Quatrini & Johnson, 2018; Wang et al., 2020; Zhang et al., 2019).

Acidithiobacillus ferrooxidans is the most studied acidophile active in the bioleaching, with more than 9000 papers in the Web of Science. Its genome (NBCI txid920) was the first to be sequenced among bioleaching microorganisms. The biological leaching of Cu from chalcopyrite has always been only partial, reaching a maximum of 60–80% over 3–4 weeks in bench-scale studies depending on the specific experimental conditions. Limited copper dissolution under mesophilic conditions is a consequence of the increased redox potential of the leach solution, which is associated with the high ferric/ferrous ratio, leading to formation of Fe(III) precipitates (Li et al., 2013; Tian et al., 2021; Zhao et al., 2019). These changes in the leach solution are known to hinder the dissolution of chalcopyrite.

Moderately thermophilic (approx. 45–60 °C) and extremely thermophilic (approx. 60–80 °C) microorganisms have faster oxidation rates and thereby bring about improvement in chalcopyrite bioleaching. Some examples

of chalcopyrite bioleaching and microbial diversity include the isolation and characterization of a novel, extremely thermoacidophilic, obligately chemolithotrophic *Acidianus sulfidivorans* (Plumb et al., 2007). This archaeon grows optimally at 74 °C and is active at a pH range of 0.4–2.2. Vilcáez et al. (2008) evaluated chalcopyrite bioleaching with three thermophiles at 65, 70, 75, and 80 °C. *Acidianus brierleyi* was the least active Fe oxidizer, suppressing the redox potential of the leach solution near the critical value of 450 $mV_{Ag/AgCl}$, thus favoring chalcopyrite leaching. *Sulfolobus metallicus* and *Metallosphaera sedula* oxidized Fe^{2+} at faster rates, thus promoting higher redox potential of the leach solution but causing lower efficiencies of chalcopyrite leaching. Iron oxidation by these thermophiles also resulted in ferric iron precipitation, which on the one hand suppresses chalcopyrite leaching and on the other hand decreases the solution redox potential, thus favoring chalcopyrite leaching. The results also demonstrated that a threshold concentration of either Fe^{2+} or Fe^{3+} is required to initiate the bioleaching of chalcopyrite.

Castro and Donati (2016) characterized a thermophilic archaeon, *Acidianus copahuensis*, which also had a low iron oxidation capacity. In bioleaching experiments, iron released from the chalcopyrite matrix remained mainly in the ferrous form because of the low oxidation activity, thus contributing to low redox potential of the leach solution. Safar et al. (2020) tested *Ac. copahuensis* further in chalcopyrite bioleaching experiments and demonstrated that initial cell adhesion on the mineral particles combined with low iron oxidation activity achieved high copper leaching, which was attributed to a low redox potential.

Liu et al. (2017) evaluated the bioleaching of a chalcopyrite concentrate sample with mixed cultures of mesophilic, moderately thermophilic, and extremely thermophilic microorganisms. Secondary covellite, chalcocite, and bornite were formed during the time course. The formation of bornite and chalcocite was observed at solution redox potentials < 500 mV_{SHE}. At > 550 mV, covellite was formed, but bornite and chalcocite were not detected. In addition, elemental S and jarosite-type precipitates were also formed; they did not appear to hinder chalcopyrite oxidation. The yields of copper leaching increased with the temperature of incubation: 59% in about 20 days at 30 °C, 78% in 16 days at 45 °C, and 85% at 65 °C in 10 days (Liu et al., 2017). Correspondingly, Hedrich et al. (2018) tested a moderately thermophilic mixed culture of *L. ferriphilum*, *Acidithiobacillus caldus,* and *Sulfobacillus* spp. for the bioleaching of a chalcopyrite concentrate sample in stirred tank temperature-controlled bioreactors. The yields of copper leaching increased with the temperature and with the lower redox potential of the leach solution.

Combinations of microbes expand the metabolic range in the bioleaching process and have been invariably more efficient than pure cultures of microbes. Pure culture work has been, however, important in elucidating oxidation steps of sulfide minerals and pathways of sulfur oxidation, iron redox shuttling, and coupling of the leaching process with biochemical energy transduction, respiratory chain activity, and physiological traits (Dopson & Okibe, 2023). Pure and mixed culture work has provided fundamental principles and premises on the limits of environmental pH, temperature, and responses to potentially toxic metals and solutes in acid leach solutions. Molecular-level and genetic studies have revealed potential to modify and manipulate properties of these microorganisms (Jung et al., 2021). These approaches are now widely used in characterization of acidophilic iron- and sulfur-oxidizing microbes, but they have yet to be integrated for commercialization of bioleaching processes.

5 Electrochemical Approaches for Chalcopyrite Dissolution

There have been ongoing discussion and interpretation of the interaction between microorganisms and the chalcopyrite substratum in the bioleaching process. Electrochemical techniques have been applied in endeavors to unravel mechanistic information and thermodynamics on bacteria–mineral interactions as it pertains to the bioleaching of chalcopyrite.

Biofilm formation impacts chalcopyrite surface and over time contributes to a passivation effect. Biofilms are typically composed of microbial cells and their extracellular polymeric substances (EPS), which can sequester metals, trap nano-size particles, and possibly also nucleate Fe(III) precipitation. Biofilms are invariably formed on mineral surfaces in bioleaching processes, causing changes in the electrochemical properties of the system (García-Meza et al., 2013; Lara et al., 2013; Bobadilla-Fazzini & Poblete-Castro, 2021). Zhao et al. (2019) and Zeng et al. (2023) elaborated on the biofilm aspects and discussed factors that are involved in bacterial attachment on chalcopyrite. Bobadilla-Fazzini and Poblete-Castro (2012) reported that biofilms of *Acidithiobacillus thiooxidans* and *Leptospirillum* spp. were not formed on chalcopyrite in stirred and laminar flow conditions. This may be a unique feature of the mixed culture as numerous other studies have proven that cell adhesion and attachment leading to biofilm layers are integral parts of the bioleaching of chalcopyrite and other sulfide minerals.

Electrochemical impedance spectroscopy (EIS) has proven a useful tool in detailing these effects. Figure 2 shows three equivalent electrical circuits (EEC) used to adjust the EIS data (Bevilaqua et al., 2004).

In the circuit A (Fig. 2a), Rs is the solution resistance and $Q_{act}(R_{ct}W)$ is connected to the electrode active region, where Q is the constant phase element composed by the admittance

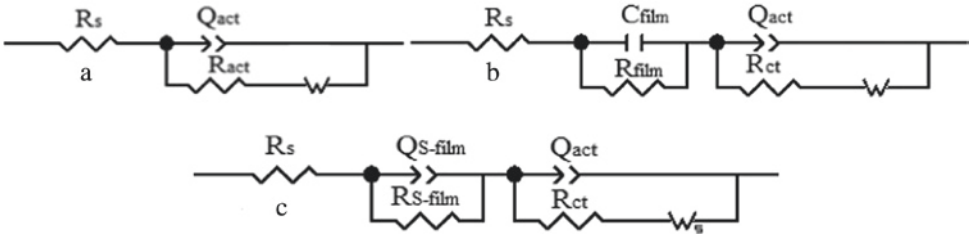

Fig. 2 Equivalent electrical circuit for EIS data: **a** 7 and 24 h in the absence and 7 h in the presence of bacteria; **b** 71 and 120 h in the absence and 24–120 h in the presence of bacteria; **c** for times longer than 120 h (Bevilaqua et al., 2004), slightly modified by the authors. Elements of the circuit: Rs, solution resistance; Q_{act}, constant phase element of the electrode active region; R_{act}, charge transfer resistance of the electrode active region; W, Warburg element that means semi-infinite linear diffusion; C_{film}, capacitance of biofilm or sulfur film partially covering the surface; R_{film}, resistance of biofilm or sulfur film partially covering the surface; $Q_{S\text{-}film}$, constant phase element of the film covering all electrode surfaces; $R_{S\text{-}film}$, resistance of the film covering almost all electrode surfaces; R_{ct}, charge transfer resistance; W_s, Warburg element, diffusion through the finite layer thickness

Yo and the exponent n of the electric double layer, both of them independent on the frequency. R_{ct} is the charge transfer resistance and W is the Warburg associated with a semi-infinite linear diffusion process. This circuit was able to describe the experimental conditions: 7 and 24 h of incubation in the absence and 7 h in the presence of bacteria. For longer times, modified circuits were proposed to represent mineral surface in part and were almost entirely covered by an adherent porous layer by compounds containing sulfur, hydroxides, biomolecules, and biomass. For immersion times between 71 and 120 h in the absence and 24–120 h in the presence of bacteria, circuit B [Rs($R_{film}C_{film}$)(Q_{act}($R_{ct}W$))] (Fig. 2b) was used where the association R-C_{film} represents the resistance and capacitance of a biofilm or sulfur film formed on part of the mineral surface. For times longer than 120 h, circuit C [(Rs($Q_{S\text{-}film}R_{S\text{-}film}$)($Q_{act}$($R_{ct}W_s$))] is shown in Fig. 2c, in which the $Q_{S\text{-}film}R_{S\text{-}film}$ sub-circuit was associated with the sulfur or biofilm covering almost entirely the electrode surface with the mass transport limited by diffusion through the film, where W_s represents a finite diffusion element (Bevilaqua et al., 2004).

Electrochemical noise analysis (ENA) has also been used to characterize bacteria–mineral interactions (Bevilaqua et al., 2006, 2007, 2011). The addition of chloride and silver ions to the bioleaching system was shown with ENA to influence the electrochemical behavior of chalcopyrite. Chloride caused an increase in the electrochemical potential and the current response of the system, thus enhancing the dissolution of chalcopyrite. Silver ions caused considerable variations in the noise resistance (R_n) values, indicating signal instability and a lack of steadiness in the leaching of chalcopyrite (Horta et al., 2009a).

The use of carbon paste electrodes (CPE) with minerals instead of massive mineral electrodes has improved reproducibility in electrochemical tests. Massive mineral electrodes are subjected to signal variability due to polishing and fracture and the lack of homogeneity (Horta et al., 2009b). The use of CPE showed a linear correlation between the mass of chalcopyrite and the charge obtained from cyclic voltammetry assays when the proportion of mineral in the CPE electrodes was between 20 and 80 wt%. By converting the noise resistance to admittance, the results of CPE studies suggested that chalcopyrite passivation was associated with slow chalcopyrite dissolution (Horta et al., 2009a). In the presence of *A. ferrooxidans* and additional chloride in the electrochemical cell, bacteria adhered to the electrode, resulting in an activated state with the influence of the two components (bacteria + Cl^- ions). This increased the admittance with a greater dispersion of the admittance points, showing a synergism between the bacteria and chloride ions in solution. Further results with CPE manufactured with solid residues from bioleaching experiments showed that chloride addition inhibited the secondary solid-phase formation on chalcopyrite. Thus, chalcopyrite dissolution was less hindered, indicating a less resistive behavior and more susceptible mineral dissolution, showing synergism between bacteria and chloride in chalcopyrite bioleaching.

The composition, structure, and other properties of chalcopyrite electrodes change during contact in the leaching solution due to precipitation, dissolution, and biomass accumulation (Kinnunen et al., 2006; Varotsis et al., 2022). The electrochemical potential of chalcopyrite electrodes decreases during these reactions; thus, it can be used to monitor the time course of the leaching process. In general, mineral electrodes with specific electrochemical potentials are used to optimize and follow mineral leaching processes.

Impedance experiments showed that the addition of Fe^{2+} decreased the capacitive arcs, suggesting the removal or absence of precipitates blocking of the electrode (Arena et al., 2016). Hydrodynamic impedance tests indicated a resistance decay of the system, which was attributed to the improved mass and ion transport, avoiding the accumulation of passivating precipitates on the electrode surface (Fig. 3). Semiconductor behavior (Crundwell, 2015) and

slow diffusion of metal ions from the interior to the chalcopyrite surface (Mikhlin et al., 2017) have also been shown to explain the slow dissolution of chalcopyrite.

The optimal redox potential range of 380–430 $mV_{Ag|AgCl|KCl(3\ mol\ L^{-1})}$ minimizes the accumulation of surface layers, because under reducing conditions, the extraction of Fe from the crystal structure and the formation of less refractory, Fe-deficient Cu-sulfides can lead to almost complete chalcopyrite dissolution (Third et al., 2000, 2002; Vilcáez & Inoue, 2009). At low redox potentials, chalcopyrite is reduced in several steps to form Cu_2S, which is relatively readily dissolved, thus improving the dissolution kinetics (Hiroyoshi et al., 2000; Gu et al., 2013; Zhao et al., 2015b, 2015d, 2017).

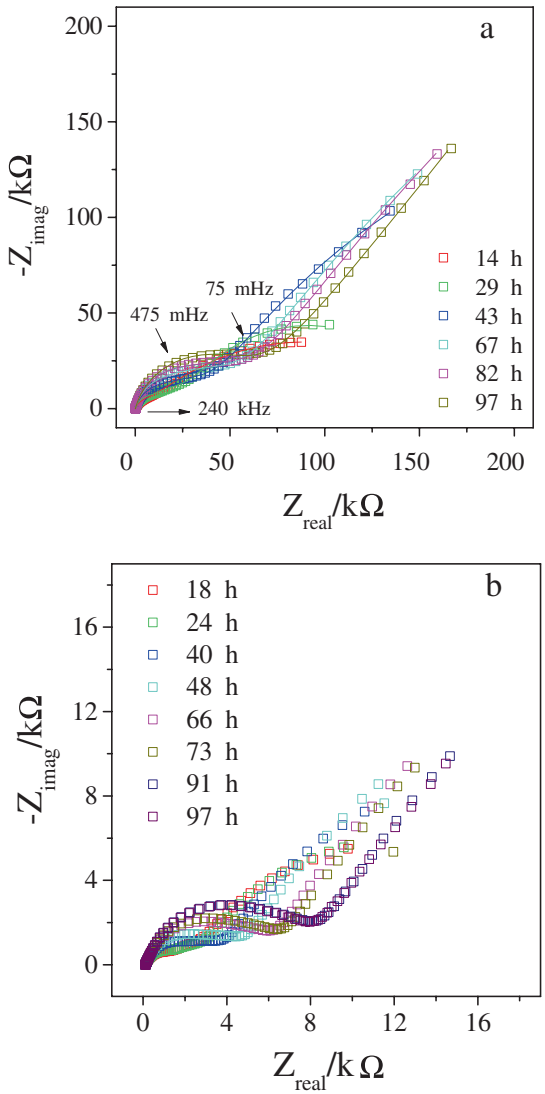

Fig. 3 Nyquist diagrams for carbon paste electrodes modified with chalcopyrite in natural aerated salts solution with 0.10 mol L^{-1} ferrous ions (**a**) (Arena et al, 2016) steady electrode (**b**) hydrodynamic electrode (1500 rpm)

Ghahremaninezhad et al. (2010, 2013) studied the chalcopyrite behavior in sulfuric acid solution in the absence of additional adding Fe^{2+} or Cu^{2+} and extended this study using XPS analysis. Based on potentiodynamic and EIS measurements, they proposed the formation of a passive layer due to the formation of metal-deficient sulfides ($Cu_{1-x}Fe_{1-y}S_2$, $y>>x$) at low potentials, and a second, copper sulfide-rich layer ($Cu_{1-x-z}S_2$), which was formed at higher potentials on the first layer as it was being dissolved. The two layers showed passive characteristics, but they started to dissolve in the range of 0.74–0.86 $V_{Ag|AgCl|KCl(3\ mol\ L^{-1})}$ leading to chalcopyrite dissolution (Ghahremaninezhad et al., 2010). The authors also studied the kinetics of Fe^{3+}/Fe^{2+} ions on anodically passivated chalcopyrite in sulfuric acid. They observed an increase in the dissolution of passivated chalcopyrite by ferric iron, which was reduced to ferrous iron and thereby lowered the redox potential (Ghahremaninezhad et al., 2012).

Processes occurring on the chalcopyrite/solution interface can be defined in relation to electrochemical mineral surface features and solution composition at specific electrochemical potentials. Mineral surfaces strongly influence the rates of chalcopyrite dissolution and the formation of intermediates and products (Lara et al., 2013; Zhao et al., 2015b). The formation of Fe(III)-phosphate on the chalcopyrite surface due to the presence of phosphate ions in the electrolyte has been noted (Lara et al., 2015). Yang et al. (2014) detected phosphorus on the surface of chalcopyrite bioleaching residues by X-ray photoelectron spectroscopy (XPS), probably as Fe(III)-phosphate precipitates at 0.60–0.65 $V_{Ag|AgCl|KClsat}$. Phosphate is used invariably in bioleach solutions as it is an important nutrient for microorganisms. Electrochemical experiments with chalcopyrite and mesophilic acidophiles and the corresponding XPS surface analyses support the formation of fractions of disulfides (S_2^{2-}), monosulfide (S^{2-}), polysulfides (S_n^{2-}) and elemental sulfur (S^0) in different proportions (Zhao et al., 2015b, 2015c). Zhao et al. (2015b) also found covellite as the main intermediate of chalcopyrite dissolution. Intermediary covellite formation during chalcopyrite oxidation has been disputed (Arce & González, 2002; Mikhlin et al., 2017). Microbial cell and EPS distribution, intermediate chemical species, and secondary solid phases on leached chalcopyrite surfaces vary spatially as well as in composition (García-Meza et al., 2013; Varotsis et al., 2022).

6 Redox Potential Control

Several reports emphasize the importance of the solution potential of the redox pairs in determining the kinetics of chalcopyrite reactions. Various hypotheses have been presented to explain this effect, and strategies for controlling

the potential have been discussed in the literature (Li et al., 2013; Zhao et al., 2019). Tian et al. (2021) summarized the effects of redox potential on the chemical leaching and bioleaching of chalcopyrite and attributed these effects to the band theory. Several chemical reactions have been proposed to describe chemical transformations of chalcopyrite and intermediates during the leaching processes. Sequences of the reactions have been characterized with electrochemical techniques and have revealed the formation of secondary sulfides (e.g., covellite, chalcocite, bornite, and other Fe-deficient sulfides) and S^0 in chemical and biological leaching experiments with chalcopyrite (Biegler & Horne, 1985; Biegler & Swift, 1979; Dutrizac & MacDonald, 1974; Elsherief, 2002; Hiroyoshi et al., 2004; Holliday & Richmond, 1990; Majuste et al., 2012; Munoz et al., 1979; Sohn & Wadsworth, 1980; Warren et al., 1982). Analyses of cathodic current (or reduction) and anodic current (or oxidation) peaks obtained with the cyclic voltammetry technique have greatly contributed to the understanding of chalcopyrite dissolution.

Many kinetic studies demonstrate that data on the chemical leaching and bioleaching of chalcopyrite in various solution compositions fit the shrinking core model. The rate limitation is a surface reaction, and the leaching over time becomes diffusion-controlled at ambient temperatures and sometimes chemical reaction-controlled at elevated temperatures (e.g., Hidalgo et al., 2019; Jordan et al., 2006; Kaplun et al., 2011; Koleini et al., 2010; Liao et al., 2020). Some chemical leaching results also indicate data fit in mixed kinetic models, changing with the time course (Ranjbar et al., 2020). Although there is only little consensus about the underlying reasons of the slow kinetics of copper extraction from chalcopyrite, poor leaching efficiency has been reported at high solution potentials, while at lower potentials (380–450 $mV_{Ag\,|\,AgCl\,|\,KClsat}$), the dissolution can reach near completion (Bevilaqua et al., 2014; Castro & Donati, 2016; Gu et al., 2013; Kametani & Aoki, 1985; Petersen & Dixon, 2006; Sandström et al., 2005; Santos et al., 2017; Third et al., 2000, 2002; Vilcáez et al., 2008; Yang et al., 2018; Zhao et al., 2015c). Studies with controlled solution potential have been carried out to better understand the role of factors that affect the bioleaching of chalcopyrite. The potential of the redox couples in the solution can be electrochemically controlled by the application of an external electrical potential with the use of electrodes or chemically using reducing agents (e.g., Na_2SO_3) or oxidizing agents (e.g., H_2O_2, O_2, $KMnO_4$). The solution potential is also influenced by the bulk microbial biomass (Li et al., 2013), although the prime redox couple in many cases is the iron shuttle, Fe^{3+}/Fe^{2+}.

Sandström et al. (2005) investigated the chemical and bacterial leaching at solution potentials maintained at 420 mV and 600 $mV_{Ag\,|\,AgCl|KClsat}$ at 65 °C, controlled with airflows and additions of $NaHSO_3$ and $KMnO_4$ solutions. Relatively high dissolution of chalcopyrite at 420 mV was observed, mainly in the chemical leaching. In the bioleaching process, a low amount of sulfur was formed because of its concurrent oxidation by bacteria at 600 mV. Because intermediate sulfur compounds were present in insignificant amounts, it was concluded that the formation of jarosite-type precipitates is key to passivation in the chalcopyrite bioleaching. Sandström et al. (2005) also noted that the dissolution rate increases with higher Cu^{2+} concentrations. Nazari and Asselin (2009) used computer simulations, based on the theory of percolation, to explain the morphology of secondary precipitates associated with the leaching of chalcopyrite in acidic ferric sulfate solution. A high copper extraction is obtained by maintaining the redox potential in the active sites of chalcopyrite within the optimal range, thus controlling the concentration and ratio of Fe^{3+} and Fe^{2+}. Without the reduction of Fe^{3+}, which slows the reaction in the active region of chalcopyrite, a Fe-deficient Cu-polysulfide passivation layer is formed, which inhibits the leaching of chalcopyrite.

Ahmadi et al. (2010) performed four types of experiments using a chalcopyrite concentrate sample in a bioreactor at 35 and 50 °C: chemical leaching, electrochemical leaching, bioleaching, and electrochemical bioleaching. In electrochemical bioleaching experiments the redox potential was controlled in the 400–450 $mV_{Ag/AgCl|KClsat}$ interval by applying an external electrical potential. The formation of a passive, Fe(III)-rich layer on chalcopyrite was limited and the highest yields of copper were obtained in these redox potential-controlled experiments (Ahmadi et al., 2010). Gericke et al. (2010) manipulated the redox potential in chalcopyrite bioreactor experiments by controlling the available oxygen concentration through aeration. About 90% copper dissolution from a chalcopyrite sample was obtained at potentials at 410–440 $mV_{Ag|AgCl}$ range, in contrast to approx. 40% extraction at 580 mV.

Velásquez-Yévenes et al. (2010) reported that the dissolution rate of chalcopyrite in 0.2 mol L^{-1} HCl with 0.5 g L^{-1} Cu^{2+} at 35 °C was strongly dependent on the solution redox potential in the range of 345–415 $mV_{Ag\,|\,AgCl\,|\,KClsat}$. The redox potential was controlled using three strategies: (i) electrochemical (a passage of an appropriate current between platinum electrodes allowing the electrode potential to be controlled to a defined value), (ii) chemical based on potentiometric titration with permanganate, and (iii) gaseous with mixtures of N_2 and O_2. The dissolution rate decreased substantially at potentials below 335 mV and above 415 mV. Chalcopyrite passivation occurring above this redox range was partially reversible if the redox potential was lowered to a more favorable value.

Gu et al. (2013) evaluated both electrochemical and bioleaching experiments using cyclic voltammetry with a

chalcopyrite electrode containing *L. ferriphilum*. Chalcocite was identified during the bioleaching of chalcopyrite at low potentials. The reductive conditions enhanced the dissolution kinetics of chalcopyrite. Jarosite was formed but was not deemed a passivating component because of its loose and porous texture. In the cyclic voltammetry test, the potential sweep followed the common path from the open-circuit potential (OCP) or 381 $mV_{Ag|AgCl|KClsat}$ to 801 mV, then to −999 $mV_{Ag|AgCl|KClsat}$ and back to the OCP value. Among the cathode peaks obtained, the reductive formation of talnakhite ($Cu_9Fe_8S_{16}$) or bornite as well as chalcocite was proposed. When the potential sweep was reversed toward the positive direction, sulfur and non-stoichiometric Cu-polysulfides such as djurleite (ideally $Cu_{31}S_{16}$, the formula varies) and digenite (Cu_9S_5) were detected.

Bevilaqua et al. (2014) evaluated the effect of the solution potential and the ratio of Fe^{3+} and Fe^{2+} concentrations on the chemical leaching and bioleaching of two types of chalcopyrite concentrates. Initial redox potentials between 350 and 600 $mV_{Ag|AgCl|KClsat}$ were adjusted with different ratios of $[Fe^{3+}]/[Fe^{2+}]$. Chalcopyrite dissolution was hindered when Fe^{2+} was completely oxidized in these experiments. The leaching rate declined when the solution potential increased to 580 mV. Enhanced copper dissolution was observed at high Fe^{2+} concentrations that suppressed the redox potential to < 370 mV.

Santos et al. (2017) reported 90% copper extraction in the chemical leaching at 200 mmol L^{-1} Fe^{2+} at redox potentials < 420 $mV_{Ag|AgCl|KClsat}$ (Fig. 4). Relatively low copper dissolution of 17% was obtained at 610 $mV_{Ag|AgCl|KClsat}$ potentials in the presence of *A. ferrooxidans*. The bacteria catalyzed the oxidation and Fe^{2+}, therefore increasing the redox potential. Under both conditions, the formation of passivating species was observed, but the dissolution of chalcopyrite was not impeded. Thus, the maintenance of a low range of redox potential in the presence of Fe^{2+} favored the leaching of chalcopyrite (Fig. 5). Factors causing the passivation of chalcopyrite leaching were not verified by Santos et al. (2017). Li et al. (2017) used synchrotron scanning photoelectron microscopy to examine chalcopyrite surfaces and residues after partial leaching at a controlled redox potential (451 $mV_{Ag|AgCl|KClsat}$), which was maintained due to the concurrent oxidation of pyrite. Intermediate sulfur species (S^{2-}, S_2^{2-}, S_n^{2-}, S^0) were identified on the surface of chalcopyrite, but their heterogeneous distribution on mineral surfaces did not indicate passivation. Evidence to date demonstrates that the bioleaching of chalcopyrite is efficient at low redox potentials and the efficiency decreases with increasing redox potential. The dominant redox shuttle comprises Fe^{2+} and Fe^{3+}, and thus, the predominance of Fe^{2+} favors the bioleaching of chalcopyrite.

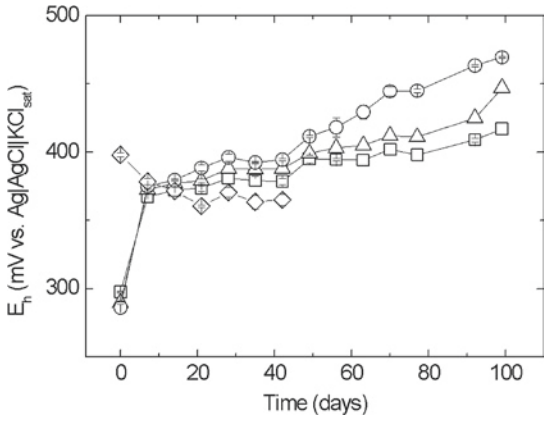

Fig. 4 Time course of copper dissolution and redox potential measurements on chalcopyrite leaching using different concentrations of ferrous ions: rhombus—0 mol L^{-1}; square—0.100 mol L^{-1}; triangle—0.200 mol L^{-1}; and circle—0.300 mol L^{-1} of ferrous ions (Santos et al., 2017)

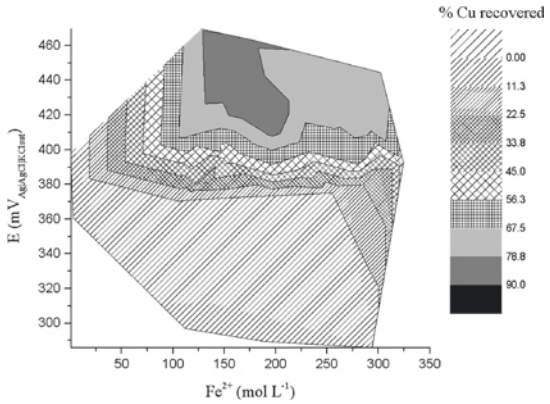

Fig. 5 Combined effect of ferrous iron concentration and redox potential on chalcopyrite dissolution under abiotic conditions (Santos et al., 2017)

Improved efficiencies would be expected with increasing Fe^{3+} concentrations, but this is not what happens at increasing redox potentials. Relatively fast rates of copper extraction have been reported for redox potentials up to a certain limit (380–480 mV versus Ag|AgCl|KCl (3 mol L^{-1}), and the presence of Cu^{2+} and Fe^{2+} also enhances the leaching of chalcopyrite (Bevilaqua et al., 2014; Biegler & Horne, 1985; Hiroyoshi et al., 1997, 2001, 2004, 2008; Sandström et al., 2005; Vilcáez et al., 2008; Nazari & Asselin, 2009; Viramontes-Gamboa et al., 2010; Velásquez-Yévenes et al., 2010; Gu et al., 2013; Zhao et al., 2015c).

In an attempt to explain the influence of solution potential and Fe^{2+}, Fe^{3+}, and Cu^{2+} on chalcopyrite leaching, Hiroyoshi et al. (2000) proposed a two-step model: chalcopyrite is initially reduced to chalcocite, followed by oxidation by Fe^{3+} and dissolved O_2 (Reactions 3–5).

$$CuFeS_2 + 3Cu^{2+} + 3Fe^{2+} \rightarrow 2Cu_2S + 4Fe^{3+}, \quad (3)$$

$$Cu_2S + 4Fe^{3+} \rightarrow 2Cu^{2+} + 4Fe^{2+} + S, \quad (4)$$

$$Cu_2S + 4H^{+} + O_2 \rightarrow 2Cu^{2+} + S + 2H_2O. \quad (5)$$

This model stipulates that the redox potential remains within a range between the Nernst potentials of the chalcopyrite reduction and chalcocite oxidation (Reactions 3–5). The dissolution of chalcopyrite would be thermodynamically inhibited if the solution potential has a value greater than the Nernst potential of the chalcopyrite reduction Reaction (3) or less than the Nernst potential of the chalcocite oxidation Reactions (4 and 5). From a thermodynamic point of view, this model may be relevant approach to approximating limitations in the bioleaching of chalcopyrite. However, studies to date show that other intermediates besides chalcocite also participate in the chalcopyrite bioleaching process.

7 Concluding Remarks

Bioleaching of Cu-sulfide ores is practiced in heaps in many locations worldwide. This technology is particularly suitable for secondary Cu-sulfides such as chalcocite and covellite as well as Cu-oxides. The primary Cu-sulfide, chalcopyrite, is refractory in these bioprocesses and requires specific process control for enhancing the extent and kinetics of the bioleaching. In the 1970's and 1980's, it was generally recognized that bioleaching could not be applied to chalcopyrite concentrates because of the slow reaction kinetics. The underlying reasons and mechanisms have been elucidated in the past couple of decades, and the acid leaching reactions aided by acidophiles can be directed toward optimization by controlling the solution redox potential and the temperature regime. Chalcopyrite electrodes in acid leaching systems can be used to monitor the oxidation state of the mineral. Pyrite electrodes can also be useful if galvanic coupling is established. Redox potential, pH, chemical oxidants, and iron- and sulfur-oxidizing microorganisms are the main controlling factors of chalcopyrite surface chemistry. These parameters change during the time course of chemical leaching and bioleaching. Active acidophiles are best employed as consortia of Fe- and S-oxidizing prokaryotes (= bacteria and archaea) for the redox-temperature-pH-ferric-ferrous-iron conditions during optimal chalcopyrite bioleaching. The formation of secondary solid phases such as (Fe(III)-precipitates, S^0, and metastable Fe-deficient Cu-sulfides accounts for the diffusion control of the leaching kinetics. Chemical and microbiological leaching of chalcopyrite yields Fe^{2+}, S^0, sulfooxyanions, and non-stoichiometric Fe- and Cu-polysulfides. Instead of a strictly chemical leaching process, the kinetics are favorable for the bioleaching, preferentially with thermophiles especially. Both the chemical leaching and bioleaching are enhanced if chalcopyrite is initially reduced to bornite and other Cu-sulfides, followed by oxidation by Fe^{3+} and dissolved O_2. The pathways of Cu, Fe, and S may be different in the chemical leaching and bioleaching. Electrochemical techniques have given insight into the sequences of leaching reactions. Analysis of the thermodynamic and electrochemical properties of chalcopyrite has presented possibilities for external control of the chalcopyrite leaching process, for example, by the process temperature, redox shuttles, aeration, galvanic coupling, and voltammetry.

Glossary

C_{film}	Capacitance of biofilm or sulfur film partially covering the surface
CPE	Carbon paste electrodes
DFT	Density functional theory
E_C	Conduction band
EEC	Equivalent electrical circuits
E_F	Fermi level
EIS	Electrochemical impedance spectroscopy
ENA	Electrochemical noise analysis
E_{redox}	Redox potential
E_V	Valence band
ΔG_f°	Standard Gibbs free energy of formation
ΔH_f°	Standard enthalpy of formation
n	Exponent
OCP	Open-circuit potential
ρ_{pulp}	Pulp density
Q	Constant phase element
$Q_{S\text{-}film}$	Constant phase element of the film covering almost entirely the electrode surface
R_{act}	Charge transfer resistance of the active region of the electrode
R_{ct}	Charge transfer resistance
R_{film}	Resistance of biofilm or sulfur film partially covering the surface
R_n	Noise resistance
rpm	Revolutions per minute
Rs	Solution resistance
$R_{S\text{-}film}$	Resistance of the film covering almost entirely the electrode surface
SAT	Saturated
SHE	Standard hydrogen electrode
U	Hubbard-type correction parameter
W	Warburg element representing a semi-infinite linear diffusion
W_s	Warburg element, representing the diffusion through a finite layer thickness

XANES	X-ray absorption near-edge spectroscopy
XPS	X-ray photoelectron spectroscopy
Yo	admittance
ZRA	Zero Resistance Ammeter mode

References

Ahmadi, A., Schaffie, M., Manafi, Z., et al. (2010). Electrochemical bioleaching of high grade chalcopyrite flotation concentrates in a stirred bioreactor. *Hydrometallurgy, 104*, 99–105. https://doi.org/10.1016/j.hydromet.2010.05.001

Ahmadi, A., Ranjbar, M., & Schaffie, M. (2013). Effect of activated carbon addition on the conventional and electrochemical bioleaching of chalcopyrite concentrates. *Geomicrobiology Journal, 30*, 237–244. https://doi.org/10.1080/01490451.2012.665152

Akcil, A., Gahan, C. S., Erust, C., et al. (2013). Influence of chloride on the chemolithotrophic acidophiles in biohydrometallurgy: A review. In K. Pramanik & J. K. Patra (Eds.), *Industrial and environmental biotechnology* (pp. 45–69). Studium Press.

Arena, F. A., Suegama, P. H., Bevilaqua, D., et al. (2016). Simulating the main stages of chalcopyrite leaching and bioleaching in ferrous ions solution: An electrochemical impedance study with a modified carbon paste electrode. *Minerals Engineering, 92*, 229–241. https://doi.org/10.1016/j.mineng.2016.03.025

Arce, E. M., & González, I. (2002). A comparative study of electrochemical behavior of chalcopyrite, chalcocite and bornite in sulfuric acid solution. *International Journal of Mineral Processing, 67*, 17–28. https://doi.org/10.1016/S0301-7516(02)00003-0

Bevilaqua, D., Acciari, H. A., Benedetti, A. V., et al. (2006). Electrochemical noise analysis of bioleaching of bornite (Cu_5FeS_4) by *Acidithiobacillus ferrooxidans*. *Hydrometallurgy, 83*, 50–54. https://doi.org/10.1016/j.hydromet.2006.03.037

Bevilaqua, D., Acciari, H. A., Benedetti, A. V., et al. (2007). Electrochemical techniques used to study bacterial-metal sulfides interactions in acidic environments. In E. R. Donati & W. Sand (Eds.), *Microbial processing of metal sulfides* (pp. 59–76). Springer.

Bevilaqua, D., Diéz-Perez, I., Fugivara, C. S., et al. (2004). Oxidative dissolution of chalcopyrite by *Acidithiobacillus ferrooxidans* analyzed by electrochemical impedance spectroscopy and atomic force microscopy. *Bioelectrochemistry, 64*, 79–84. https://doi.org/10.1016/j.bioelechem.2004.01.006

Bevilaqua, D., Lahti-Tommila, H., Garcia Júnior, O., et al. (2014). Bacterial and chemical leaching of chalcopyrite concentrates as affected by the redox potential and ferric/ferrous iron ratio at 22 °C. *International Journal of Mineral Processing, 132*, 1–7. https://doi.org/10.1016/J.MINPRO.2014.08.008

Bevilaqua, D., Lahti, H., Suegama, P. H., et al. (2013). Effect of Na-chloride on the bioleaching of a chalcopyrite concentrate in shake flasks and stirred tank bioreactors. *Hydrometallurgy, 138*, 1–13. https://doi.org/10.1016/j.hydromet.2013.06.008

Bevilaqua, D., Suegama, P. H., Garcia Júnior, O., et al. (2011). Electrochemical studies of sulphide minerals in the presence and absence of *Acidithiobacillus ferrooxidans*. In L. G. Sobral, D. M. Oliveira, & C. E. G. Souza (Eds.), *Biohydrometallurgy processes: A practical approach* (pp. 143–167). CETEM/MCT.

Biegler, T., & Horne, M. D. (1985). The electrochemistry of surface oxidation of chalcopyrite. *Journal of the Electrochemical Society, 132*, 1363–1369. https://doi.org/10.1149/1.2114117

Biegler, T., & Swift, D. A. (1979). Anodic electrochemistry of chalcopyrite. *Journal of Applied Electrochemistry, 9*, 545–554. https://doi.org/10.1007/BF00610940

Bobadilla-Fazzini, R. A., & Poblete-Castro, I. (2021). Biofilm formation is crucial for efficient copper bioleaching from bornite under mesophilic conditions: unveiling the lifestyle and catalytic role of sulfur-oxidizing bacteria. *Frontiers in Microbiology, 12*, 761997. https://doi.org/10.3389/fmicb.2021.761997

Bott, A. W. (1998). Electrochemistry of semiconductors. *Current Separations, 27*, 87–91

Castro, C., & Donati, E. (2016). Effects of different energy sources on cell adhesion and bioleaching of a chalcopyrite concentrate by extremophilic archaeon *Acidianus copahuensis*. *Hydrometallurgy, 162*, 49–56. https://doi.org/10.1016/j.hydromet.2016.02.014

Crundwell, F. K. (2015). The semiconductor mechanism of dissolution and the pseudo-passivation of chalcopyrite. *Canadian Metallurgical Quarterly, 54*, 279–288. https://doi.org/10.1179/1879139515Y.0000000007

Crundwell, F. K. (1988). The influence of the electronic structure of solids on the anodic dissolution and leaching of semiconducting sulphide minerals. *Hydrometallurgy, 21*, 155–190. https://doi.org/10.1016/0304-386X(88)90003-5

Dopson, M., Holmes, D. S., Lazcano, M., et al. (2017). Multiple osmotic stress responses in *Acidihalobacter prosperus* result in tolerance to chloride ions. *Frontiers in Microbiology, 7*, 2132. https://doi.org/10.3389/fmicb.2016.02132

Dopson, M., & Okibe, N. (2023). Biomining microorganisms: Diversity and *modus operandi*. In D. B. Johnson, C. G. Bryan, M. Schlömann, & F. F. Roberto (Eds.), *Biomining technologies: Extracting and recovering metals from ores and waste* (pp. 89–110). Springer Nature. https://doi.org/10.1007/978-3-031-05382-5_5

Dutrizac, J. E. (1991). Ferric ion leaching of chalcopyrites from different localities. *Journal of Electronic Materials, 20*, 303–309. https://doi.org/10.1007/BF02816001

Dutrizac, J. E. (1978). The kinetics of dissolution of chalcopyrite in ferric ion media. *Metallurgical Transactions B, 9*, 431–439. https://doi.org/10.1007/BF02654418

Dutrizac, J. E. (1989). Elemental sulphur formation during the ferric sulphate leaching of chalcopyrite. *Canadian Metallurgical Quarterly, 28*, 337–344. https://doi.org/10.1179/cmq.1989.28.4.337

Dutrizac, J. E., & MacDonald, R. J. C. (1974). The kinetics of dissolution of covellite in acidified ferric sulphate solutions. *Canadian Metallurgical Quarterly, 13*, 423–433. https://doi.org/10.1179/cmq.1974.13.3.423

Elsherief, A. E. (2002). The influence of cathodic reduction, Fe^{2+} and Cu^{2+} ions on the electrochemical dissolution of chalcopyrite in acidic solution. *Minerals Engineering, 15*, 215–223. https://doi.org/10.1016/S0892-6875(01)00208-4

Fontana, M. G. (1987). *Corrosion engineering* (3rd ed.). McGraw-Hill.

García-Meza, J. V., Fernández, J. J., Lara, R. H., et al. (2013). Changes in biofilm structure during the colonization of chalcopyrite by *Acidithiobacillus thiooxidans*. *Applied Microbiology and Biotechnology, 97*, 6065–6075. https://doi.org/10.1007/s00253-012-4420-6

Gericke, M., Govender, Y., & Pinches, A. (2010). Tank bioleaching of low-grade chalcopyrite concentrates using redox control. *Hydrometallurgy, 104*, 414–419. https://doi.org/10.1016/j.hydromet.2010.02.024

Ghahremaninezhad, A., Asselin, E., & Dixon, D. G. (2010). Electrochemical evaluation of the surface of chalcopyrite during dissolution in sulfuric acid solution. *Electrochimica Acta, 55*, 5041–5056. https://doi.org/10.1016/j.electacta.2010.03.052

Ghahremaninezhad, A., Dixon, D. G., & Asselin, E. (2012). Kinetics of the ferric-ferrous couple on anodically passivated chalcopyrite ($CuFeS_2$) electrodes. *Hydrometallurgy, 125–126*, 42–49. https://doi.org/10.1016/j.hydromet.2012.05.004

Ghahremaninezhad, A., Dixon, D. G., & Asselin, E. (2013). Electrochemical and XPS analysis of chalcopyrite ($CuFeS_2$) dissolution in sulfuric acid solution. *Electrochimica Acta, 87*, 97–112. https://doi.org/10.1016/j.electacta.2012.07.119

Gu, G., Hu, K., Zhang, X., et al. (2013). The stepwise dissolution of chalcopyrite bioleached by *Leptospirillum ferriphilum*. *Electrochimica Acta, 103*, 50–57. https://doi.org/10.1016/j.electacta.2013.04.051

Hidalgo, T., Kuhar, L., Beinlich, A., et al. (2019). Kinetics and mineralogical analysis of copper dissolution from a bornite/chalcopyrite composite sample in ferric-chloride and methanesulfonic-acid solutions. *Hydrometallurgy, 188*, 140–156. https://doi.org/10.1016/j.hydromet.2019.06.009

Hiroyoshi, N., Hirota, M., Hirajima, T., et al. (1997). A case of ferrous sulfate addition enhancing chalcopyrite leaching. *Hydrometallurgy, 47*, 37–45. https://doi.org/10.1016/S0304-386X(97)00032-7

Hiroyoshi, N., Kitagawa, H., & Tsunekawa, M. (2008). Effect of solution composition on the optimum redox potential for chalcopyrite leaching in sulfuric acid solutions. *Hydrometallurgy, 91*, 144–149. https://doi.org/10.1016/j.hydromet.2007.12.005

Hiroyoshi, N., Kuroiwa, S., Miki, H., et al. (2004). Synergistic effect of cupric and ferrous ions on active-passive behavior in anodic dissolution of chalcopyrite in sulfuric acid solutions. *Hydrometallurgy, 74*, 103–116. https://doi.org/10.1016/j.hydromet.2004.01.003

Hiroyoshi, N., Miki, H., Hirajima, T., et al. (2001). Enhancement of chalcopyrite leaching by ferrous ions in acidic ferric sulfate solutions. *Hydrometallurgy, 60*, 185–197. https://doi.org/10.1016/S0304-386X(00)00155-9

Hiroyoshi, N., Miki, H., Hirajima, T., & Tsunekawa, M. (2000). Model for ferrous-promoted chalcopyrite leaching. *Hydrometallurgy, 57*, 31–38. https://doi.org/10.1016/S0304-386X(00)00089-X

Holliday, R. I., & Richmond, W. R. (1990). An electrochemical study of the oxidation of chalcopyrite in acidic solution. *Journal of Electroanalytical Chemistry, 288*, 83–98. https://doi.org/10.1016/0022-0728(90)80027-4

Horta, D. G., Acciari, H. A., Bevilaqua, D., et al. (2009a). The effect of chloride ions and *A. ferrooxidans* on the oxidative dissolution of the chalcopyrite evaluated by electrochemical noise analysis (ENA). *Advances in Materials Research, 71–73*, 397–400. https://doi.org/10.4028/WWW.SCIENTIFIC.NET/AMR.71-73.397

Horta, D. G., Bevilaqua, D., Acciari, H. A., et al. (2009b). Optimization of the use of carbon paste electrodes (CPE) for electrochemical study of the chalcopyrite. *Quimica Nova, 32*, 1734–1738. https://doi.org/10.1590/S0100-40422009000700010

Huynh, D., Giebner, F., Kaschabek, S. R., et al. (2019). Effect of sodium chloride on *Leptospirillum ferriphilum* DSM 14647^T and *Sulfobacillus thermosulfidooxidans* DSM 9293^T: Growth, iron oxidation activity and bioleaching of sulfidic metal ores. *Minerals Engineering, 138*, 52–59. https://doi.org/10.1016/j.mineng.2019.04.033

Johnson, D. B., & Quatrini, R. (2020). Acidophile microbiology in space and time. *Current Issues in Molecular Biology, 39*, 63–76. https://doi.org/10.21775/cimb.039.063

Jordan, H., Sanhueza, A., Gautier, V., et al. (2006). Electrochemical study of the catalytic influence of *Sulfolobus metallicus* in the bioleaching of chalcopyrite at 70 °C. *Hydrometallurgy, 83*, 55–62. https://doi.org/10.1016/j.hydromet.2006.03.038

Jung, H., Inaba, Y., & Banta, S. (2021). Genetic engineering of the acidophilic chemolithoautotroph *Acidithiobacillus ferrooxidans*. *Trends in Biotechnology, 40*, 677–692. https://doi.org/10.1016/j.tibtech.2021.10.004

Kaplun, K., Li, J., Kawashima, N., et al. (2011). Cu and Fe chalcopyrite leach activation energies and the effect of added Fe^{3+}. *Geochimica et Cosmochimica Acta, 75*, 5865–5878. https://doi.org/10.1016/j.gca.2011.07.003

Kametani, H., & Aoki, A. (1985). Effect of suspension potential on the oxidation rate of copper concentrate in a sulfuric acid solution. *Metallurgical Transactions B, 16*, 695–705. https://doi.org/10.1007/BF02667506

Khaleque, H. N., Kaksonen, A. H., Boxall, N. J., & et al. (2018). Chloride ion tolerance and pyrite bioleaching capabilities of pure and mixed halotolerant, acidophilic iron- and sulfur-oxidizing cultures. *Minerals Engineering, 120*, 87–93. https://doi.org/10.1016/j.mineng.2018.02.025

Khoshkhoo, M., Dopson, M., Shchukarev, A., et al. (2014). Chalcopyrite leaching and bioleaching: An X-ray photoelectron spectroscopic (XPS) investigation on the nature of hindered dissolution. *Hydrometallurgy, 149*, 220–227. https://doi.org/10.1016/j.hydromet.2014.08.012

Kinnunen, P.H.-M., Heimala, S., Riekkola-Vanhanen, M.-L., et al. (2006). Chalcopyrite concentrate leaching with biologically produced ferric sulphate. *Bioresource Technology, 97*, 1727–1734. https://doi.org/10.1016/j.biortech.2005.07.016

Klauber, C. (2008). A critical review of the surface chemistry of acidic ferric sulphate dissolution of chalcopyrite with regards to hindered dissolution. *International Journal of Mineral Processing, 86*, 1–17. https://doi.org/10.1016/j.minpro.2007.09.003

Klauber, C., Parker, A., Van Bronswijk, W., et al. (2001). Sulphur speciation of leached chalcopyrite surfaces as determined by X-ray photoelectron spectroscopy. *International Journal of Mineral Processing, 62*, 65–94. https://doi.org/10.1016/S0301-7516(00)00045-4

Koleini, S. M. J., Jafarian, M., Abdollahy, M., et al. (2010). Galvanic leaching of chalcopyrite in atmospheric pressure and sulfate media: Kinetic and surface studies. *Industrial and Engineering Chemistry Research, 49*, 5997–6002. https://doi.org/10.1021/ie100017u

Lara, R. H., García-Meza, J. V., González, I., et al. (2013). Influence of the surface speciation on biofilm attachment to chalcopyrite by *Acidithiobacillus thiooxidans*. *Applied Microbiology and Biotechnology, 97*, 2711–2724. https://doi.org/10.1007/s00253-012-4099-8

Lara, R. H., Vazquez-Arenas, J., Ramos-Sanchez, G., et al. (2015). Experimental and theoretical analysis accounting for differences of pyrite and chalcopyrite oxidative behaviors for prospective environmental and bioleaching applications. *Journal of Physical Chemistry C, 119*, 18364–18379. https://doi.org/10.1021/acs.jpcc.5b05149

Latorre, M., Cortés, M. P., Travisany, D., et al. (2016). The bioleaching potential of a bacterial consortium. *Bioresource Technology, 218*, 659–666. https://doi.org/10.1016/j.biortech.2016.07.012

Liao, R., Wang, X., Yang, B., et al. (2020). Catalytic effect of silver-bearing solid waste on chalcopyrite bioleaching: A kinetic study. *Journal of Central South University, 27*, 1395–1403. https://doi.org/10.1007/s11771-020-4375-1

Li, Y., Kawashima, N., Li, J., et al. (2013). A review of the structure, and fundamental mechanisms and kinetics of the leaching of chalcopyrite. *Advances in Colloid and Interface Science, 197–198*, 1–32. https://doi.org/10.1016/j.cis.2013.03.004

Li, Y., Qian, G., Brown, P. L., et al. (2017). Chalcopyrite dissolution: Scanning photoelectron microscopy examination of the evolution of sulfur species with and without added iron or pyrite. *Geochimica et Cosmochimica Acta, 212*, 33–47. https://doi.org/10.1016/j.gca.2017.05.016

Liu, H.-C., Xia, J.-I., Nie, Z.-Y., et al. (2017). Comparative study of S, Fe and Cu speciation transformation during chalcopyrite bioleaching by mixed mesophiles and mixed thermophiles. *Minerals Engineering, 106*, 22–32. https://doi.org/10.1016/j.mineng.2017.01.013

Liu, Q., & Li, H. (2011). Electrochemical behaviour of chalcopyrite ($CuFeS_2$) in $FeCl_3$ solution at room temperature under differential stress. *International Journal of Mineral Processing, 98*, 82–88. https://doi.org/10.1016/j.minpro.2010.10.010

Lv, X., Wang, J., & Zeng, X., et al. (2021). Cooperative extraction of metals from chalcopyrite by bio-oxidation and chemical oxidation. *Geochemistry, 81*, 125772. https://doi.org/10.1016/j.chemer.2021.125772

Mahmoud, A., Cézac, P., Hoadley, A. F. A., et al. (2017). A review of sulfide minerals microbially assisted leaching in stirred tank reactors. *International Biodeterioration and Biodegradation, 119*, 118–146. https://doi.org/10.1016/j.ibiod.2016.09.015

Majuste, D., Ciminelli, V. S. T., Osseo-Asare, K., et al. (2012). Electrochemical dissolution of chalcopyrite: Detection of bornite by synchrotron small angle X-ray diffraction and its correlation with the hindered dissolution process. *Hydrometallurgy, 111–112*, 114–123. https://doi.org/10.1016/j.hydromet.2011.11.003

Martins, F. L., & Leão, V. A. (2023). Chalcopyrite bioleaching in chloride media: A mini-review. *Hydrometallurgy, 216*, 105995. https://doi.org/10.1016/j.hydromet.2022.105995

Martins, F. L., Patto, G. B., & Leão, V. A. (2019). Chalcopyrite bioleaching in the presence of high chloride concentrations. *Journal of Chemical Technology and Biotechnology, 94*, 2333–2344. https://doi.org/10.1002/jctb.6028

Memming, R. (2015). *Semiconductor electrochemistry* (2nd ed.). Wiley-VCH Verlag.

Méndez, A., Álvarez, M. L., Fidalgo, J. M., et al. (2022). Biomass-derived activated carbon as catalyst in the leaching of metals from a copper sulfide concentrate. *Minerals Engineering, 183*, 107594. https://doi.org/10.1016/j.mineng.2022.107594

Mikhlin, Y., Nasluzov, V., Romanchenko, A., et al. (2017). Layered structure of the near-surface region of oxidized chalcopyrite ($CuFeS_2$): Hard X-ray photoelectron spectroscopy, X-ray absorption spectroscopy and DFT+*U* studies. *Physical Chemistry Chemical Physics, 19*, 2749–2759. https://doi.org/10.1039/c6cp07598c

Mikhlin, Y. L., Tomashevich, Y. V., Asanov, I. P., et al. (2004). Spectroscopic and electrochemical characterization of the surface layers of chalcopyrite ($CuFeS_2$) reacted in acidic solutions. *Applied Surface Science, 225*, 395–409. https://doi.org/10.1016/j.apsusc.2003.10.030

Moya-Beltrán, A., Simón Beard, S., Rojas-Villalobos, C., et al. (2021). Genomic evolution of the class Acidithiobacillia: Deep-branching Proteobacteria living in extreme acidic conditions. *ISME Journal, 15*, 3221–3238. https://doi.org/10.1038/s41396-021-00995-x

Munoz, P. B., Miller, J. D., & Wadsworth, M. E. (1979). Reaction mechanism for the acid ferric sulfate leaching of chalcopyrite. *Metallurgical Transactions B, B10*, 149–158. https://doi.org/10.1007/BF02652458

Nasluzov, V., Shor, A., Romanchenko, A., et al. (2019). DFT + *U* and low-temperature XPS studies of Fe-depleted chalcopyrite ($CuFeS_2$) surfaces: A focus on polysulfide species. *Journal of Physical Chemistry C, 123*, 21031–21041. https://doi.org/10.1021/acs.jpcc.9b06127

Natarajan, K. A., & Kumari, A. (2014). Role of applied potentials on bioleaching of chalcopyrite concentrate and growth of *Acidithiobacillus ferrooxidans*. *Minerals and Metallurgical Processing, 31*, 215–222.

Nava, D., González, I., Leinen, D., et al. (2008). Surface characterization by X-ray photoelectron spectroscopy and cyclic voltammetry of products formed during the potentiostatic reduction of chalcopyrite. *Electrochimica Acta, 53*, 4889–4899. https://doi.org/10.1016/j.electacta.2008.01.088

Nazari, G., & Asselin, E. (2009). Morphology of chalcopyrite leaching in acidic ferric sulfate media. *Hydrometallurgy, 96*, 183–188. https://doi.org/10.1016/j.hydromet.2008.09.004

Nicol, M. (2021). The initial stages of the dissolution of chalcopyrite in chloride solutions: Validity of mixed potential model and comparison with sulfate solutions. *Hydrometallurgy, 204*, 105721. https://doi.org/10.1016/j.hydromet.2021.105721

Nicol, M., Miki, H., & Zhang, S. (2017). The anodic behaviour of chalcopyrite in chloride solutions: Voltammetry. *Hydrometallurgy, 171*, 198–205. https://doi.org/10.1016/j.hydromet.2017.05.016

Nicol, M., & Zhang, S. (2017). The anodic behaviour of chalcopyrite in chloride solutions: Potentiostatic measurements. *Hydrometallurgy, 167*, 72–80. https://doi.org/10.1016/j.hydromet.2016.10.008

Nicol, M. J. (2017a). The use of impedance measurements in the electrochemistry of the dissolution of sulfide minerals. *Hydrometallurgy, 169*, 99–102. https://doi.org/10.1016/j.hydromet.2016.12.013

Nicol, M. J. (2017b). The anodic behaviour of chalcopyrite in chloride solutions: Overall features and comparison with sulfate solutions. *Hydrometallurgy, 169*, 321–329. https://doi.org/10.1016/j.hydromet.2017.02.009

Nicol, M. J. (2019). The electrochemistry of chalcopyrite in alkaline solutions. *Hydrometallurgy, 187*, 134–140. https://doi.org/10.1016/j.hydromet.2019.05.016

Nuñez, H., Moya-Beltrán, A., Covarrubias, P. C., et al. (2017). Molecular systematics of the genus *Acidithiobacillus*: Insights into the phylogenetic structure and diversification of the taxon. *Frontiers in Microbiology, 8*, 30. https://doi.org/10.3389/fmicb.2017.00030

Nyembwe, K. J., Fosso-Kankeu, E., Wanders, F., & et al. (2018). Mineralogical observation made during the kinetic dissolution study of chalcopyrite mineral in sulphate media under free pH at room temperature. In *10th International conference on advances in science, engineering, technology and healthcare* (pp. 148–152) Cape Town, South Africa. https://doi.org/10.17758/eares4.eap1118240

O'Connor, G. M., & Eksteen, J. J. (2020). A critical review of the passivation and semiconductor mechanisms of chalcopyrite leaching. *Minerals Engineering, 154*, 106401. https://doi.org/10.1016/j.mineng.2020.106401

Olvera, O. G., Quiroz, L., Dixon, D. G., et al. (2014). Electrochemical dissolution of fresh and passivated chalcopyrite electrodes. Effect of pyrite on the reduction of Fe^{3+} ions and transport processes within the passive film. *Electrochimica Acta, 127*, 7–19. https://doi.org/10.1016/j.electacta.2014.01.165

Osseo-Asare, K. (1992). Semiconductor electrochemistry and hydrometallurgical dissolution processes. *Hydrometallurgy, 29*, 61–90. https://doi.org/10.1016/0304-386X(92)90006-L

Parker, A., Klauber, C., Kougianos, A., et al. (2003). An X-ray photoelectron spectroscopy study of the mechanism of oxidative dissolution of chalcopyrite. *Hydrometallurgy, 71*, 265–276. https://doi.org/10.1016/S0304-386X(03)00165-8

Pathnak, P. A., Morrison, L., et al. (2017). Catalytic potential of selected metal ions for bioleaching, and potential techno-economic and environmental issues: A critical review. *Bioresource Technology, 229*, 211–221. https://doi.org/10.1016/j.biortech.2017.01.001

Petersen, J., & Dixon, D. G. (2006). Competitive bioleaching of pyrite and chalcopyrite. *Hydrometallurgy, 83*, 40–49. https://doi.org/10.1016/j.hydromet.2006.03.036

Peters, E. (1977). The electrochemistry of sulphide minerals. In J. O'M Bockris, D. A. J. Rand, & B. J. Welch (Eds.), *Trends in electrochemistry* (pp. 267–290) Plenum Publishing.

Plumb, J. J., Haddad, C. M., Gibson, J. A. E., et al. (2007). *Acidianus sulfidivorans* sp. nov., an extremely acidophilic, thermophilic archaeon isolated from a solfatara on Lihir Island, Papua New Guinea, and emendation of the genus description. *International Journal of Systematic and Evolutionary Microbiology, 57*, 1418–1423. https://doi.org/10.1099/ijs.0.64846-0

Quatrini, R., & Johnson, D. B. (2018). Microbiomes in extremely acidic environments: Functionalities and interactions that allow survival and growth of prokaryotes at low pH. *Current Opinion in Microbiology, 43*, 139–147. https://doi.org/10.1016/j.mib.2018.01.011

Ram, R., Coyle, V. E., Bond, A. M., et al. (2020). A scanning electrochemical microscopy (SECM) study of the interfacial solution chemistry at polarised chalcopyrite ($CuFeS_2$) and chalcocite (Cu_2S). *Electrochemistry Communications, 115*, 106730. https://doi.org/10.1016/j.elecom.2020.106730

Ranjbar, M., Hamghavandi, M. R., Fazaelipoor, M. H., et al. (2020). Development of a kinetic model of bacterial dissolution of copper concentrate. *Mining, Metallurgy and Exploration, 37*, 345–353. https://doi.org/10.1007/s42461-019-00114-7

Sadeghieh, S. M., Ahmadi, A., & Hosseini, M. R. (2020). Effect of water salinity on the bioleaching of copper, nickel and cobalt from the sulphidic tailing of Golgohar iron mine, Iran. *Hydrometallurgy, 198*, 105503. https://doi.org/10.1016/j.hydromet.2020.105503

Safar, C., Castro, C., & Donati, E. (2020). Importance of initial interfacial steps during chalcopyrite bioleaching by a thermoacidophilic archaeon. *Microorganisms, 8*, 1009. https://doi.org/10.3390/microorganisms8071009

Sandström, Å., Shchukarev, A., & Paul, J. (2005). XPS characterisation of chalcopyrite chemically and bio-leached at high and low redox potential. *Minerals Engineering, 18*, 505–515. https://doi.org/10.1016/j.mineng.2004.08.004

Santos, A. L. A., Arena, F. A., Benedetti, A. V., & et al. (2017). Effect of redox potential on chalcopyrite dissolution imposed by addition of ferrous ions. *Eclética Química, 42*, 40. https://doi.org/10.26850/1678-4618eqj.v42.1.2017.p40-50

Sasaki, K., Takatsugi, K., & Tuovinen, O. H. (2012). Spectroscopic analysis of the bioleaching of chalcopyrite by *Acidithiobacillus caldus*. *Hydrometallurgy, 127–128*, 116–120. https://doi.org/10.1016/j.hydromet.2012.07.013

Sedriks, A. J. (1996). *Corrosion of stainless steel* (2nd ed.). John Wiley & Sons.

Sohn, H.-J., & Wadsworth, M. E. (1980). Reduction of chalcopyrite with SO_2 in the presence of cupric ions. *Journal of Metals, 32*, 18–22. https://doi.org/10.1007/BF03354577

Tanne, C., & Shippers, A. (2021). Electrochemical investigation of microbially and galvanically leached chalcopyrite. *Hydrometallurgy, 202*, 105603–105611. https://doi.org/10.1016/j.hydromet.2021.105603

Third, K. A., Cord-Ruwisch, R., & Watling, H. R. (2000). Role of iron-oxidizing bacteria in stimulation or inhibition of chalcopyrite bioleaching. *Hydrometallurgy, 57*, 225–233. https://doi.org/10.1016/S0304-386X(00)00115-8

Third, K. A., Cord-Ruwisch, R., & Watling, H. R. (2002). Control of the redox potential by oxygen limitation improves bacterial leaching of chalcopyrite. *Biotechnology and Bioengineering, 78*, 433–441. https://doi.org/10.1002/bit.10184

Tian, Z., Li, H., Wei, Q., & et al. (2021). Effects of redox potential on chalcopyrite leaching: An overview. *Minerals Engineering, 172*, 107135. https://doi.org/10.1016/j.mineng.2021.107135

Toledo, A. G. R., Tayar, S. P., Arena, F. A., et al. (2022). New insights into oxidative-reductive leaching of chalcopyrite concentrate using a central composite factorial design. *Minerals Engineering, 180*, 107467. https://doi.org/10.1016/j.mineng.2022.107467

Uhlig, H. H. (1978). History of passivity, experiments and theories. In R. P. Frankenthal & J. Kruger (Eds.), *Passivity of metals* (pp. 1–28). The Electrochemical Society.

Vakylabad, A. B., Nazari, S., & Darezereshki, E. (2022). Bioleaching of copper from chalcopyrite ore at higher NaCl concentrations. *Minerals Engineering, 175*, 107281. https://doi.org/10.1016/j.mineng.2021.107281

Varotsis, C., Tselios, C., Yiannakkos, K. A., Andreou, C., et al. (2022). Application of double-pulse laser-induced breakdown spectroscopy (DP-LIBS), Fourier transform infrared micro-spectroscopy and Raman microscopy for the characterization of copper sulfides. *RSC Advances, 12*, 631–639. https://doi.org/10.1039/D1RA07189K

Velásquez-Yévenes, L., Nicol, M., & Miki, H. (2010). The dissolution of chalcopyrite in chloride solutions. *Hydrometallurgy, 103*, 108–113. https://doi.org/10.1016/j.hydromet.2010.03.001

Vilcáez, J., & Inoue, C. (2009). Mathematical modeling of thermophilic bioleaching of chalcopyrite. *Minerals Engineering, 22*, 951–960. https://doi.org/10.1016/j.mineng.2009.03.001

Vilcáez, J., Suto, K., & Inoue, C. (2008). Bioleaching of chalcopyrite with thermophiles: Temperature–pH–ORP dependence. *International Journal of Mineral Processing, 88*, 37–44. https://doi.org/10.1016/j.minpro.2008.06.002

Viramontes-Gamboa, G., Peña-Gomar, M. M., & Dixon, D. G. (2010). Electrochemical hysteresis and bistability in chalcopyrite passivation. *Hydrometallurgy, 105*, 140–147. https://doi.org/10.1016/j.hydromet.2010.08.012

Viramontes-Gamboa, G., Rivera-Vasquez, B. F., & Dixon, D. G. (2007). The active-passive behavior of chalcopyrite: Comparative study between electrochemical and leaching responses. *Journal of the Electrochemical Society, 154*, C299. https://doi.org/10.1149/1.2721782

Viramontes-Gamboa, G., Rivera-Vásquez, B. F., & Dixon, D. G. (2006). The active-to-passive transition of chalcopyrite. *ECS Transactions, 2*, 165–175. https://doi.org/10.1149/1.2196007

Wang, X., Ma, L., Wu, J., et al. (2020). Effective bioleaching of low-grade copper ores: Insights from microbial cross experiments. *Bioresource Technology, 308*, 123273. https://doi.org/10.1016/j.biortech.2020.123273

Wang, L., Yin, S., Deng, B., et al. (2022). Copper sulfides leaching assisted by acidic seawater-based media: Ionic strength and mechanism. *Minerals Engineering, 175*, 107286. https://doi.org/10.1016/j.mineng.2021.107286

Warren, G. W., Wadsworth, M. E., & El-Raghy, S. M. (1982). Passive and transpassive anodic behavior of chalcopyrite in acid solutions. *Metallurgical Transactions B, 13*, 571–579. https://doi.org/10.1007/BF02650014

Watling, H. R. (2013). Chalcopyrite hydrometallurgy at atmospheric pressure: 1. Review of acidic sulfate, sulfate–chloride and sulfate–nitrate process options. *Hydrometallurgy, 140*, 163–180. https://doi.org/10.1016/j.hydromet.2013.09.013

Weisener, C. G., Smart, R. S. C., & Gerson, A. R. (2003). Kinetics and mechanisms of the leaching of low Fe sphalerite. *Geochimica et Cosmochimica Acta, 67*, 823–830. https://doi.org/10.1016/S0016-7037(02)01276-0

Yang, B., Gan, M., Luo, W., et al. (2017). Synergistic catalytic effects of visible light and graphene on bioleaching of chalcopyrite. *RSC Advances, 7*, 49838–49848. https://doi.org/10.1039/C7RA10015A

Yang, B., Luo, W., Wang, X., et al. (2020). The use of biochar for controlling acid mine drainage through the inhibition of chalcopyrite biodissolution. *Science of the Total Environment, 737*, 139485. https://doi.org/10.1016/j.scitotenv.2020.139485

Yang, C., Qin, W., Zhao, H., et al. (2018). Mixed potential plays a key role in leaching of chalcopyrite: Experimental and theoretical analysis. *Industrial and Engineering Chemistry Research, 57*, 1733–1744. https://doi.org/10.1021/acs.iecr.7b02051

Yang, Y., Harmer, S., & Chen, M. (2014). Synchrotron X-ray photoelectron spectroscopic study of the chalcopyrite leached by moderate thermophiles and mesophiles. *Minerals Engineering, 69*, 185–195. https://doi.org/10.1016/j.mineng.2014.08.011

Yang, Y., Liu, W., Gao, X., et al. (2019). An XAS study of silver species evolution in silver-catalysed chalcopyrite bioleaching. *Hydrometallurgy, 186*, 252–259. https://doi.org/10.1016/j.hydromet.2019.04.023

Yu, P. H., Hansen, C. K., & Wadsworth, M. E. (1973). A kinetic study of the leaching of chalcopyrite at elevated temperatures. *Metallurgical Transactions, 4*, 2137–2144. https://doi.org/10.1007/BF02643279

Zammit, C. M., Mangold, S., Jonna, V. R., & et al. (2012). Bioleaching in brackish waters—Effect of chloride ions on the acidophile population and proteomes of model species. *Applied Microbiology and Biotechnology, 93*, 319–329. https://doi.org/10.1007/s00253-011-3731-3

Zeng, W., Liu, Z., Amanze, C., et al. (2023). In situ detection of Cu^{2+}, Fe^{3+} and Fe^{2+} ions at the microbe-mineral interface during bioleaching of chalcopyrite by moderate thermophiles. *Minerals Engineering, 191*, 107936. https://doi.org/10.1016/j.mineng.2022.107936

Zhang, X., Liu, X., Li, L., et al. (2019). Phylogeny, divergent evolution, and speciation of sulfur-oxidizing *Acidithiobacillus* populations. *BMC Genomics, 20*, 438. https://doi.org/10.1186/s12864-019-5827-6

Zhao, H., Huang, X., Wang, J., et al. (2017). Comparison of bioleaching and dissolution process of *p*-type and *n*-type chalcopyrite. *Minerals Engineering, 109*, 153–161. https://doi.org/10.1016/j.mineng.2017.03.013

Zhao, H., Wang, J., Gan, X., et al. (2015a). Effects of pyrite and bornite on bioleaching of two different types of chalcopyrite in the presence of *Leptospirillum ferriphilum*. *Bioresource Technology, 194*, 28–35. https://doi.org/10.1016/j.biortech.2015.07.003

Zhao, H., Wang, J., Qin, W., et al. (2015b). Electrochemical dissolution process of chalcopyrite in the presence of mesophilic microorganisms. *Minerals Engineering, 71*, 159–169. https://doi.org/10.1016/j.mineng.2014.10.025

Zhao, H., Wang, J., Qin, W., et al. (2015c). Surface species of chalcopyrite during bioleaching by moderately thermophilic bacteria. *Transactions of Nonferrous Metals Society of China, 25*, 2725–2733. https://doi.org/10.1016/S1003-6326(15)63897-3

Zhao, H., Wang, J., Yang, C., & et al. (2015d). Effect of redox potential on bioleaching of chalcopyrite by moderately thermophilic bacteria: An emphasis on solution compositions. *Hydrometallurgy, 151*, 141–150. https://doi.org/10.1016/j.hydromet.2014.11.009

Zhao, H., Zhanga, Y., Zhang, X., et al. (2019). The dissolution and passivation mechanism of chalcopyrite in bioleaching: An overview. *Minerals Engineering, 136*, 140–154. https://doi.org/10.1016/j.mineng.2019.03.014

Zhao, C., Yang, B., Liao, R., et al. (2022). Combined effect and mechanism of visible light and Ag^{+} on chalcopyrite bioleaching. *Minerals Engineering, 175*, 107283. https://doi.org/10.1016/j.mineng.2021.107283

Zheng, X.-F., Nie, Z.-Y., Jiang, Q, & et al. (2021). The mechanism by which FeS_2 promotes the bioleaching of $CuFeS_2$: An electrochemical and DFT study. *Mineral Engineering, 173*, 107233. https://doi.org/10.1016/j.mineng.2021.107233